DOI: 10.1002/cphc.201200529

Quantifying Large Effects of Framework Flexibility on Diffusion in MOFs: CH_4 and CO_2 in ZIF-8

Emmanuel Haldoupis, Taku Watanabe, Sankar Nair, and David S. Sholl*[a]

Metal organic frameworks (MOFs) have recently emerged as a new class of nanoporous materials, and have generated great interest as adsorbents and membranes for gas separations and other applications.[1] To use MOFs for membrane separations, it is desirable to select materials that possess high selectivity based on strong molecular sieving behavior.[2] The large (currently >5000) and rapidly growing number of synthesized MOFs creates a challenge in efficiently finding high-performance materials. Computational methods that can be applied to large libraries of materials have been developed to predict molecular adsorption and diffusion in MOFs.[3] These methods, like the great majority of atomistic models of MOFs, approximate the MOF as a rigid structure.

A small number of computational studies have explored the influence of framework flexibility on molecular diffusion in MOFs.[4] In large-pore materials, the impact of flexibility on diffusion is relatively small. This has been shown, for example, for benzene in IRMOF-1.[4a] Recent calculations for methane (CH_4) in ZIF-8 by Hertäg et al.,[4d] however, suggest that framework flexibility can significantly enhance molecular diffusion relative to a rigid framework. In the latter case, diffusion of CH_4 (kinetic diameter 3.8 Å) in rigid ZIF-8 is slow because the diameter of the rigid ZIF-8 window (3.42 Å) is too small to allow hopping between the cages of ZIF-8.[3a]

An important drawback of the above calculations is that different force fields for the MOF atoms can lead to significantly different calculated CH_4 diffusivities, thereby requiring parameterization of force fields for each new material of interest. It is highly desirable to have efficient and reliable methods that can assess the role of MOF framework flexibility in molecular diffusion without relying on time-consuming parameterization of force fields. Herein, we introduce an approach that achieves this goal by efficiently combining ab initio molecular dynamics (AIMD) calculations of a MOF framework with classical atomistic modeling of adsorbate diffusion. AIMD does not require specification of a force field for the MOF degrees of freedom. As such, this approach is suitable for treating chemically diverse collections of nanoporous materials such as MOFs and zeolites. We illustrate our approach by examining the diffusion of spherical and nonspherical gas molecules in ZIF-8, an important and widely studied MOF material. This allows us to compare our results to a number of recent experiments on ZIF-8 membranes.[5]

The time scales that can be accessed by AIMD are short relative to the times needed to probe diffusion of adsorbed molecules. The framework vibrational modes resulting in framework flexibility effects, however, are accessible by AIMD. The basis of our approach, therefore, is to use AIMD to gather information about the flexible framework in the absence of adsorbed molecules, and then to use this information to describe adsorbate diffusion with a classical atomistic model.

To illustrate our approach, AIMD calculations for ZIF-8 at 300 K were performed using the Vienna ab initio simulation package (VASP)[7] with the Perdew–Burke–Ernzerhof (PBE) functional. The electron kinetic energy cutoff was set to 400 eV, and *k*-space was sampled at the Γ point. The initial structure was obtained by geometry optimization of the unit cell. The optimized geometry is a cubic unit cell with the lattice parameter of 17.137 Å. During AIMD, the lattice constant was kept fixed at the DFT-optimized value (17.137 Å), but atom positions were unconstrained. A Nosé thermostat with Nosé mass of 1.28×10^{-28} a.u. was used to maintain the temperature at 300 K. ZIF-8 structural configurations were recorded at intervals of 1 fs during a 1 ps trajectory. Each configuration includes eight distinct windows separating two cages in ZIF-8. We modified our earlier computational methods[3a] for pore-size analysis to efficiently measure the pore-limiting diameter for each of the 8000 window configurations generated by this calculation. The resulting distribution of window diameters is shown in Figure 1, which also shows the window size for the experimental crystal structure and a Gaussian fit of the distri-

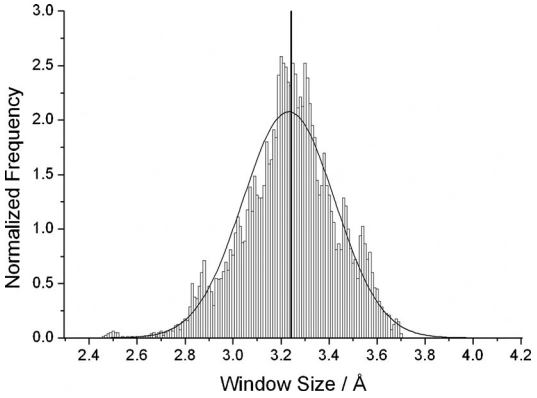

Figure 1. Distribution of the 8000 window sizes in ZIF-8 observed over a 1 ps ab initio MD simulation, normalized to have an area of unity. The vertical line shows the window size of the ZIF-8 framework from the diffraction-based structure solution,[6] and the smooth line is a Gaussian fit of the distribution.

[a] *E. Haldoupis, Dr. T. Watanabe, Prof. S. Nair, Prof. D. S. Sholl*
School of Chemical & Biomolecular Engineering
Georgia Institute of Technology
Atlanta, GA, 30332-0100 (USA)
E-mail: david.sholl@chbe.gatech.edu

Supporting information for this article is available on the WWW under http://dx.doi.org/10.1002/cphc.201200529.

bution. It is clear that diffusion of molecules with sizes slightly larger than the nominal diameter of the crystal structure will be strongly affected by the tail of the distribution corresponding to wider windows.

We now consider the prediction of molecular diffusivity in the infinite dilution limit in the ensemble of structures obtained from AIMD. The self, corrected and transport diffusivities are all equal under infinite dilution conditions[8] and therefore for simplicity we refer to it simply as diffusivity from now on. We studied five gases approximated as spherical particles (CH_4, H_2, He, Ar, and Xe) using the gas–gas Lennard-Jones potentials listed in Table S1 (Supporting Information). Gas–MOF interactions were defined by pairwise Lennard-Jones potentials.[3a] Our earlier methods efficiently determine the activation energy for diffusion of spherical molecules once a force field defining the molecule–MOF interactions is available.[3a] This approach is used here to compute the activation energy for each molecule through each of the 8000 ZIF-8 windows sampled by AIMD. To connect this information with diffusion properties, we calculated the hopping rate of each species through each window using transition state theory (TST) by means of methods described earlier.[3a] The net diffusivity of a species is then given by[9] $D=(1/6)k_{avg}\alpha^2$, where k_{avg} is the average hopping rate with respect to the distribution of windows in the structure and α is the cage-to-cage hopping distance. To obtain accurate results using TST, we fit the pre-exponential factor in the TST expression for the hopping rate to classical molecular dynamics (MD) data for the five gases in a rigid model of ZIF-8 (Supporting Information).

Figure 2 shows the calculated diffusivities at 300 K for CH_4, H_2, He, Ar, and Xe in ZIF-8 using several representations of the MOF structure. Three of these calculations used rigid approximations to ZIF-8 based on the experimental structure: 1) determined using neutron powder diffraction (NPD) measurements,[6] 2) the geometry-optimized DFT structure, and 3) a structure defined by a time average of the atomic positions in our AIMD data. The latter approximation was suggested recently by Krishna et al. as a possible means of examining the role of framework vibrations on diffusion in nanopores.[10] For the rigid framework models, the diffusivities were calculated applying TST using the eight windows present in the structure. For molecules smaller than the crystallographic window size of ZIF-8 (H_2, He, and Ar), the differences between these three approximations have only a minor impact on diffusion. For larger molecules, however, the small structural differences between these rigid structures change the predicted diffusivity by orders of magnitude. When the full distribution of window sizes is used, the computed diffusivity of CH_4 and Xe is orders of magnitude larger than in any of the rigid approximations including the time-averaged structure. For CH_4 (Xe), the predicted diffusivity at 300 K when flexibility is accounted for is 5 (13) orders of magnitude higher than the result from the rigid material using the experimental crystal structure.

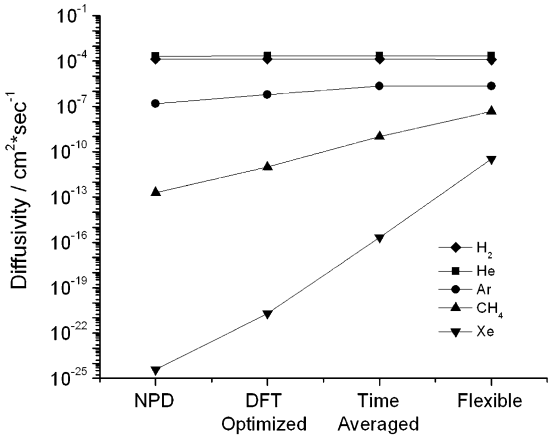

Figure 2. Diffusivities in the infinite dilution limit for five gases with four representations of the ZIF-8 framework at 300 K.

Apart from the quantification of the profound effect of framework flexibility, another finding that emerges from Figure 2 is that the window diameter does not give a complete description of the hopping rate through a window. The rigid NPD and DFT-optimized structures yield almost identical pore-limiting diameters (3.242 and 3.248 Å, a difference of 0.19%), but the difference in diffusivity for CH_4 (Xe) between these two structures is ~50 (~5000). These large differences exist because the transition-state energy defined by the windows differs by considerably more than would be expected from the window size alone. Because our calculations use the full potential energy surface for the diffusing molecules, they correctly account for these important effects. We verified that these differences are associated with variation in the transition-state energies, and not the energy minimum associated with molecular adsorption in ZIF-8 cages. An implication of this observation is that the Henry's constants for molecular adsorption are only weakly affected by the inclusion of framework flexibility (Supporting Information).

The calculations described above only give results at 300 K. It is obviously useful to probe the temperature dependence of diffusion while incorporating framework flexibility. We tackled this task without performing additional AIMD calculations as follows. First, we assumed that the probability of observing a window with diameter d is $P(d)\sim\exp(-E(d)/kT)$, where E is the energy associated with distorting the window to have diameter d relative to the minimum-energy state. Once this probability distribution is known at one temperature (300 K), we can readily predict the distribution at other temperatures. For simplicity we used the Gaussian distribution fitted to our 300 K AIMD data (Figure 1), although the distribution from AIMD can be directly used as well. Second, we developed a mathematical function for each guest molecule that relates the observed window size with the average diffusion activation energy for windows of the specified size (Supporting Information). Once these activation energies are defined, we used TST as described above to determine the net diffusivity of each gas. There can be variation in the activation energies for windows with a fixed size, as already discussed. However, the diffusivity for CH_4 at 300 K from our distribution-fitting approach differs from the result of the full AIMD distribution by $<5\%$.

The temperature dependence of the diffusivity of CH_4, Ar, and Xe in ZIF-8 obtained from our calculations is shown in

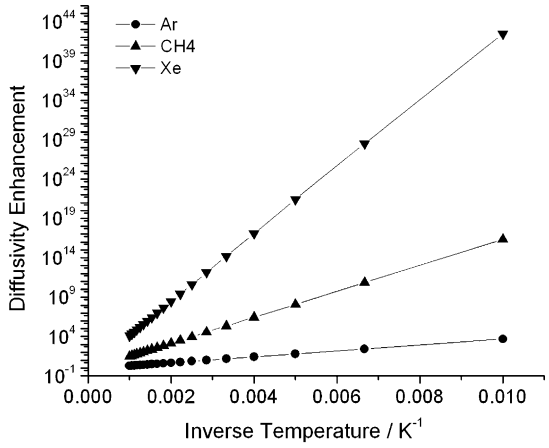

Figure 3. Ratio of diffusivities in flexible ZIF-8 to rigid ZIF-8 for Ar, CH_4 and Xe as a function of temperature.

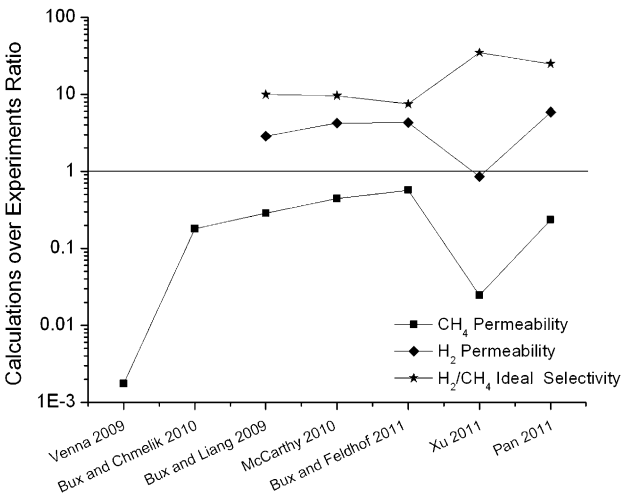

Figure 4. Comparison of experimental measurements of CH_4 and H_2 permeability through ZIF-8 membranes at room temperature with our calculations using the flexible model of ZIF-8 at 300 K.

Figure 3. The effect of flexibility on H_2 and He is negligible, so these species are not shown. For the larger species, the effect of flexibility becomes more pronounced at lower temperatures. A useful way to quantify this effect is to determine the effective activation energy of $D_{flexible}/D_{rigid}$, from Figure 3. This is the reduction in the overall activation energy for diffusion due to framework flexibility. For CH_4 (Xe), this change in activation energy was found to be 32 (82) kJ mol^{-1}.

It is helpful to compare our predictions with experimental measurements of molecular permeation through ZIF-8. Since 2009, there have been multiple reports of gas permeation measurements in polycrystalline ZIF-8 membranes.[5] All these reports have measured permeances for CH_4 and H_2 at room temperature, except in the work by Venna et al.[5b] and Bux et al.[5c] (Yao et al.[5h]), which did not give results for H_2 (CH_4). We used the reported permeances and membrane thicknesses (Supporting Information) to obtain permeability values that can be directly compared with our calculated results. At infinite dilution, the permeability is equal to the product of the diffusion coefficient and the Henry's constant.[11]

Figure 4 compares the reported experimental values for permeability and ideal selectivity to our flexible-framework predictions. The ideal selectivity is the ratio of the single component permeabilities. There is considerable variation among the experimental permeabilities, presumably due to differences in the microstructure and defect density in the fabricated membranes. The four experiments with the lowest permeabilities are in reasonable agreement with each other, and probably represent the closest approximation to defect-free membranes that can currently be achieved. For these cases, the agreement between the experiments and our calculated values is quite good. In all cases, our calculations underpredict (overpredict) the CH_4 (H_2) permeance, and as a result the H_2/CH_4 ideal selectivity predicted by our calculations is larger than experiment by roughly a factor of 10. The inevitable presence of even a small number of defects in the experimental membranes will reduce the H_2/CH_4 selectivity relative to defect-free ZIF-8, so it is reasonable that the calculations give a larger selectivity than experiments. To put this level of agreement into a more meaningful perspective, the same predictions made with a rigid approximation for the ZIF-8 framework lead to a CH_4 permeability (H_2/CH_4 selectivity) that is 3.3 million (7.4 million) times greater than the average experimental values. It is also worth noting that we underpredict the CH_4 diffusivity measured by infrared microscopy (IRM) by Bux et al.[5c] by a factor of 21. Clearly, including the effects of framework flexibility is critical to quantitatively predicting the properties of CH_4 in this material, and allows a drastic improvement in the capability to predict diffusion in MOFs.

We also examined CO_2 diffusion in ZIF-8 to examine the applicability of our approach to non-spherical adsorbates. Similar to the situation in small-pore zeolites,[12] the transition state (TS) for cage-to-cage hopping of CO_2 in ZIF-8 is not the narrowest region of the pore. A TST-based calculation for CO_2 would therefore require accurately locating the TS for each AIMD snapshot. Fortunately, this complication can be avoided by directly observing cage-to-cage hopping rates with classical MD because CO_2 diffuses sufficiently rapidly in ZIF-8. We performed classical MD of CO_2 diffusing in the infinite dilution limit in a large number of ZIF-8 structures taken from our AIMD calculations and used these results to determine the CO_2 hopping rate averaged over all snapshots and cages. Details of these simulations are listed in the Supporting Information.

We calculated the CO_2 diffusivity at 300 K for the NPD, DFT optimized and flexible model for ZIF-8 and compared it with the experimentally measured diffusivity using infrared microscopy by Bux et al.[5c] We also compared our results from three recent classical simulation studies using different flexible force fields for ZIF-8.[4c,e,f] Figure 5 shows the ratio of the calculated diffusivities to the experimental value. The diffusivities used for this comparison are listed in Table S2. Most of the results are in reasonable agreement with the experimental value, although one is ~25 times larger. Our treatment of flexibility gives a diffusivity ~8.3 times larger than using the rigid DFT optimized structure. Unlike the spherical adsorbates we considered

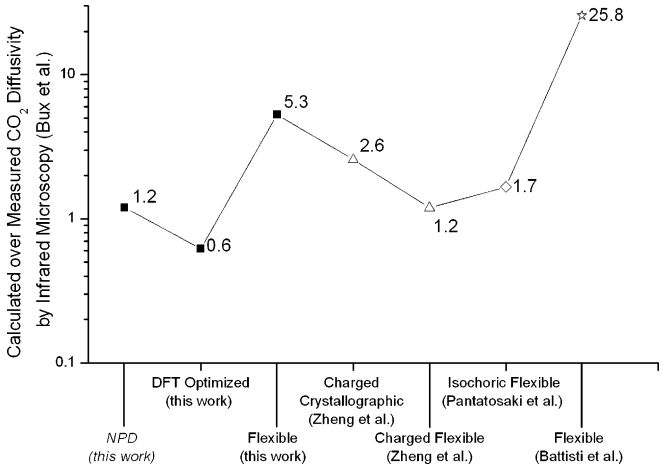

Figure 5. Comparison between calculated CO_2 diffusivities using different framework models and forcefields and the experimentally measured value using infrared microscopy by Bux et al.[5c] Filled (open) symbols are from our calculations (classical calculations from earlier work).

above, the rigid DFT structure shows slightly slower diffusion than the rigid NPD structure, supporting the claim above that the TS for diffusion for non-spherical adsorbates is not simply located at the narrowest portion of the pore.

When Zheng et al. included framework flexibility in their classical simulations, the diffusivity of CO_2 was reduced by a small amount compared to calculations with a rigid structure.[4f] It is unclear, however, if their force field reliably reproduces the degrees of freedom in the vibrating framework that have the greatest effect on the TS for CO_2 diffusion. Overall, the variability in the diffusivities obtained from flexible framework simulations with differing force fields means that we can conclude that our AIMD-based results are in reasonable agreement with the fully classical methods, but a more precise conclusion about which result among the methods in Figure 5 is more reliable is difficult to justify.

There are several assumptions and limitations in the method as presently demonstrated that would be useful to address in future work. For example, it would be useful to extend our approach to finite adsorbate loadings. This should be possible using relatively well-developed molecular simulation methods. It will also be useful to perform calculations to probe our assumption that the dynamics of the framework in the vicinity of the adsorbate TS are approximately decoupled from the adsorbate.

In summary, we have introduced a new approach to calculating the diffusivity of molecules in nanoporous materials that accounts for framework flexibility but does not require a force field for the motion of the nanoporous framework. This approach, which combines ab initio and classical simulations, is well-suited to examining a wide range of materials, including MOFs and zeolites. We have illustrated this approach by describing the diffusion of six gases through ZIF-8. Our calculations show that accounting for framework flexibility leads to orders-of-magnitude improvements in accuracy of the predictions for CH_4 as well as reasonable agreement with membrane experiments. Our results also show that there are cases in which framework flexibility is unimportant, namely for molecules smaller than the pore-limiting diameter, as well as cases where framework flexibility plays a critical role. The latter class includes all cases in which a separation is achieved by a strong "molecular sieving" effect. As a result, the ability to include framework flexibility in assessing the performance of MOFs will be vital in developing these materials for separations and other applications in which diffusion plays an important role.

Acknowledgements

This work was supported by the ConocoPhillips company (E.H., S.N., and D.S.) and by DOE ARPA-E (T.W., S.N., and D.S.).

Keywords: diffusion · membranes · metal-organic framework · molecular dynamics · molecular modeling

[1] a) S. T. Meek, J. A. Greathouse, M. D. Allendorf, *Adv. Mater.* **2011**, *23*, 249 – 267; b) J.-R. Li, R. J. Kuppler, H.-C. Zhou, *Chem. Soc. Rev.* **2009**, *38*, 1477 – 1504; c) R. J. Kuppler, D. J. Timmons, Q.-R. Fang, J.-R. Li, T. A. Makal, M. D. Young, D. Yuan, D. Zhao, W. Zhuang, H.-C. Zhou, *Coord. Chem. Rev.* **2009**, *253*, 3042 – 3066.

[2] S. Keskin, T. M. Van Heest, D. S. Sholl, *ChemSusChem* **2010**, *3*, 879 – 891.

[3] a) E. Haldoupis, S. Nair, D. S. Sholl, *J. Am. Chem. Soc.* **2010**, *132*, 7528 – 7539; b) E. Haldoupis, S. Nair, D. S. Sholl, *J. Am. Chem. Soc.* **2012**, *134*, 4313 – 4323; c) C. E. Wilmer, M. Leaf, C. Y. Lee, O. K. Farha, B. G. Hauser, J. T. Hupp, R. Q. Snurr, *Nat. Chem.* **2012**, *4*, 83 – 89.

[4] a) S. Amirjalayer, M. Tafipolsky, R. Schmid, *Angew. Chem.* **2007**, *119*, 467 – 470; *Angew. Chem. Int. Ed.* **2007**, *46*, 463 – 466; b) K. Seehamart, T. Nanok, R. Krishna, J. M. van Baten, T. Remsungnen, S. Fritzsche, *Microporous Mesoporous Mater.* **2009**, *125*, 97 – 100; c) A. Battisti, S. Taioli, G. Garberoglio, *Microporous Mesoporous Mater.* **2011**, *143*, 46 – 53; d) L. Hertäg, H. Bux, J. Caro, C. Chmelik, T. Remsungnen, M. Knauth, S. Fritzsche, *J. Membr. Sci.* **2011**, *377*, 36 – 41; e) E. Pantatosaki, G. Megariotis, A.-K. Pusch, C. Chmelik, F. Stallmach, G. K. Papadopoulos, *J. Phys. Chem. C* **2012**, *116*, 201 – 207; f) B. Zheng, M. Sant, P. Demontis, G. B. Suffritti, *J. Phys. Chem. C* **2012**, *116*, 933 – 938; g) Q. Yang, H. Jobic, F. Salles, D. Kolokolov, V. Guillerm, C. Serre, G. Maurin, *Chem. Eur. J.* **2011**, *17*, 8882 – 8889.

[5] a) H. Bux, F. Liang, Y. Li, J. Cravillon, M. Wiebcke, J r. Caro, *J. Am. Chem. Soc.* **2009**, *131*, 16000 – 16001; b) S. R. Venna, M. A. Carreon, *J. Am. Chem. Soc.* **2010**, *132*, 76 – 78; c) H. Bux, C. Chmelik, J. M. van Baten, R. Krishna, J. Caro, *Adv. Mater.* **2010**, *22*, 4741 – 4743; d) M. C. McCarthy, V. Varela-Guerrero, G. V. Barnett, H.-K. Jeong, *Langmuir* **2010**, *26*, 14636 – 14641; e) H. Bux, A. Feldhoff, J. Cravillon, M. Wiebcke, Y.-S. Li, J. Caro, *Chem. Mater.* **2011**, *23*, 2262 – 2269; f) Y. Pan, Z. Lai, *Chem. Commun.* **2011**, *47*, 10275 – 10277; g) G. Xu, J. Yao, K. Wang, L. He, P. A. Webley, C.-s. Chen, H. Wang, *J. Membr. Sci.* **2011**, *385 – 386*, 187 – 193; h) J. Yao, D. Dong, D. Li, L. He, G. Xu, H. Wang, *Chem. Commun.* **2011**, *47*, 2559 – 2561.

[6] H. Wu, W. Zhou, T. Yildirim, *J. Am. Chem. Soc.* **2007**, *129*, 5314 – 5315.

[7] G. Kresse, J. Furthmüller, *Phys. Rev. B* **1996**, *54*, 11169 – 11186.

[8] D. S. Sholl, *Acc. Chem. Res.* **2006**, *39*, 403 – 411.

[9] R. L. June, A. T. Bell, D. N. Theodorou, *J. Phys. Chem.* **1991**, *95*, 8866 – 8878.

[10] R. Krishna, J. M. van Baten, *J. Phys. Chem. C* **2010**, *114*, 18017 – 18021.

[11] S. Keskin, D. S. Sholl, *Langmuir* **2009**, *25*, 11786 – 11795.

[12] S. E. Jee, D. S. Sholl, *J. Am. Chem. Soc.* **2009**, *131*, 7896 – 7904.

Received: June 29, 2012
Published online on July 18, 2012

